



# Study of the repeated collapsibility of undisturbed loess in Guyuan, China

Haiman Wang<sup>1,2</sup> · Wankui Ni<sup>1,2</sup> · Haisong Liu<sup>1,2</sup> · Miansong Huang<sup>3</sup> · Kangze Yuan<sup>1,2</sup> · Lan Li<sup>1,2</sup> · Xiangning Li<sup>1,2</sup>

Received: 15 January 2020 / Accepted: 24 May 2021 / Published online: 11 June 2021  
© Springer-Verlag GmbH Germany, part of Springer Nature 2021

## Abstract

At present, the international evaluation method of loess collapsibility only evaluates loess once collapses, but some scholars have found that loess is characterized with the phenomenon of repeated collapsibility under certain conditions. To explore the characteristics of repeated collapsibility of loess and to find a simple and feasible method for evaluating repeated collapsibility of loess, this paper selects soil samples with different water content for repeated compression tests. Loess is a typical structural soil, and its structure is significantly weakened by water and pressure. This paper combines three main parameters influencing the structure of loess to define a comprehensive physical index and explores the relationship between the comprehensive physical index and the structural yield strength of loess under repeated collapsibility. Using the structural yield strength of loess to normalize the compression curve during repeated collapse, a method for evaluating repeated collapsing of loess has been proposed. This method combines the compression index of loess with the basic physical parameters of loess, which is more suitable for evaluating the repeated collapsibility of loess. By comparing the calculation results with the measured results, it was determined that this method has high accuracy. This method was used to calculate the coefficient of collapsibility of Guyuan loess, and the results show that loess with a moisture content of < 17% can collapse twice.

**Keywords** Undisturbed loess · Comprehensive physical index · Collapsibility evaluation · Repeated collapse

## Introduction

Loess is a typical structured soil characterized by water sensitivity and collapsibility (Lutenegger 1981; Gao 1988; Jiang et al. 2014; Xie et al. 2017, 2018; Li 2018). The collapsibility of loess is closely related to its structure (Lutenegger 1981; Gao 1988), and it can collapse under its own weight and/or surcharge loads when flooded (Kim and Kang 2013; Lv et al. 2014; Liang et al. 2018). In recent years, the implementation

of the “Western Development” and “The Belt and Road Initiative” strategies has made considerable progress in the construction of infrastructure in Northwest China. The northwestern part of China is mostly covered with thick loess, and in construction engineering, the collapsing of loess is inevitable. Engineering accidents caused by the collapse of loess are common (Rogers et al. 1994; Mihalache and Buscarnera 2015; Mei et al. 2019), so research on the collapsibility of loess has become particularly important.

Guyuan is located on the northwestern edge of the Loess Plateau, and the thickness of the collapsible loess is 35 m. As a pilot city for the construction of sponge city on the Loess Plateau, Guyuan must consider the collapsibility of loess during the project. The purpose of the sponge city is to introduce part of the rainwater into the ground, so some existing buildings could collapse again. The demolition and reconstruction of old buildings caused by the construction of the sponge city will also cause the repeated collapse of the loess foundation. Therefore, the repetitive collapsibility of loess plays a significant role in the sponge city project; thus, the studies of repeated collapsibility of loess are becoming more significant. Several studies on the collapsibility of

✉ Wankui Ni  
niwankui@chd.edu.cn

<sup>1</sup> College of Geological Engineering and Geomatics, Chang’an University, Xi’an, Shaanxi, 710054 People’s Republic of China

<sup>2</sup> Key Lab of Western Geological Resources and Geoengineering Under Ministry of Education, Chang’an University, Xi’an, Shaanxi, 710054 People’s Republic of China

<sup>3</sup> Ningxia Capital Sponge City Construction & Development CO, LTD2, Guyuan, Ningxia, 756000 People’s Republic of China

loess have been performed (Delage et al. 1996; Romero and Simms 2008; Yuan and Wang 2009; Liu et al. 2013; Shao et al. 2018), while only a few have investigated repeated collapsibility. Sun and Liu (2000) conducted a large-scale ( $10 \times 10$  m) field test in Gansu, on a site that has been irrigated more than 150 times since it was built in 1972. However, after being immersed for 40 days, the self-collapse was still 42.5 cm. Based on this, loess will continue to collapse as long as there is residual collapsibility.

At present, the global method of estimating loess collapsibility can evaluate collapsibility only once, mainly by obtaining a collapsibility coefficient, which requires significant time and numerous samples. In order to investigate the law of repeated collapsibility of loess and to develop a simple and feasible method for evaluating the coefficient of repeated loess collapsibility, this paper performed repeated collapsibility tests on samples with different water content in Guyuan area. Based on the analysis of the compression characteristics of loess and its relationship with structure, a comprehensive physical index reflecting the structure of loess was defined. In addition, this paper established a method for uniformly describing the compression curve of loess to calculate the corresponding deformation index and proposed a method for evaluating the collapsibility of loess using the basic physical index.

## Materials and methods

### Study area and samples

The loess soil samples used in the present study are from Guyuan City in China (Fig. 1). The soil at the sampling site is  $Q_3$  loess (known as Malan loess in China) with yellow color. All loess samples were carefully collected at a depth of 2 m below the ground. A total of 13 samples were collected on site, and all samples were carved into a cylinder approximately 10 cm in diameter and 20 cm in height and

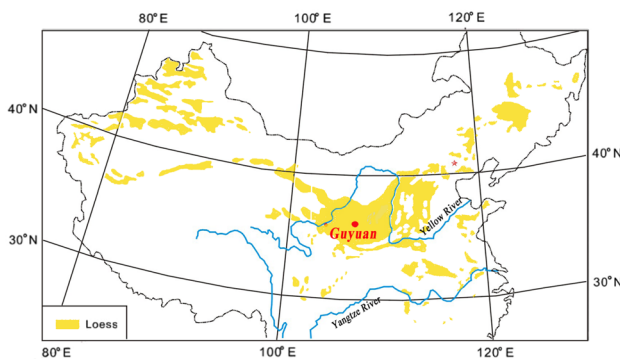


**Fig. 1** Location map showing the loess distribution in China and sampling site (Dijkstra 2001; Hao et al. 2010)

**Table 1** Physical properties of loess samples used in the present study

Property	Value
Dry density $\rho_d$ (g/cm <sup>3</sup> )	1.20–1.24
Natural water content $w_0$ (%)	16.9–17.1
Initial void ratio $e_0$	1.08–1.12
Specific gravity $G_s$	2.69
Liquid limit $w_L$ (%)	26.6
Plastic limit $w_p$ (%)	17.4
Particle size distribution	
Sand 0.075–2 mm (%)	9.05
Silt 0.002–0.075 mm (%)	84.88
Clay <0.002 mm (%)	6.07
Soluble salt (mmol/kg)	
CaCO <sub>3</sub>	1.91
CaSO <sub>4</sub>	0.35
MgSO <sub>4</sub>	2.24
NaHCO <sub>3</sub>	4.04
K <sub>2</sub> SO <sub>4</sub>	0.5
KCl	1.33
NaCl	1.77

kept in a sample bucket and sealed with paraffin. Prior to transport to laboratory, the sample buckets were packed in wooden boxes that were filled and covered with straw to avoid any disturbances. Some basic physical properties of the loess samples are listed in Table 1. At least two groups of parallel tests were conducted for each index. The soil particle size distribution test was performed using a Betsize 2000 laser particle size analyzer, which showed that the loess samples consisted mainly of silt (approximately 84.88%), with some clay (approximately 6.07%) (Table 1; Fig. 2). In addition, the soluble salt content of loess was determined by the method described in the Chinese National Standard (CNS, MOWR 2019).

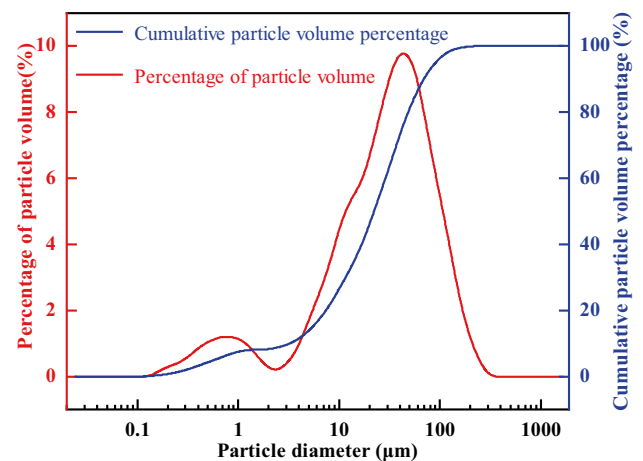


**Fig. 2** Particle size distribution of the examined loess samples

### Test design and methods

To achieve the research objective, confined compression tests of undisturbed loess with different water content (8%, 17%, 28%, and 37%) were performed, and the corresponding tested pressures were 50 kPa, 100 kPa, 150 kPa, 200 kPa, 300 kPa, 400 kPa, 500 kPa, 600 kPa, 700 kPa, and 800 kPa. Compression tests were performed using a high-pressure consolidation device. After application of each load level, the deformation per hour was less than 0.01 mm compared to the stability standard (ASTM International 2003). The height of the sample was recorded, and the next load level was applied. The pressure increased step by step until the end of the test. After the sample was stabilized at the last pressure level, it was injected into the consolidation device with water and unloaded after the sample was stabilized again. After the first test, the samples were naturally dried to the target moisture content in order to be used in the second test. Taking as an example a sample with moisture content of 8%, the test steps are shown in Fig. 3. The samples in this test had a height of 20 mm and an area of 100 cm<sup>2</sup>. Methods for preparing the undisturbed samples with different water content are given below.

For samples that required humidification, the “titration plus water method” was adopted, i.e., the required amount of water is evenly and slowly released on the samples surface. If the amount of released water was large, the water dripping was performed gradually. The increase in water content in each stage of the dripping process did not exceed 5%. The water used in the experiment was distilled water in order to prevent the introduction of other ions that could affect the experimental results. The “natural air drying” method was adopted for hygroscopic samples. For this, the samples

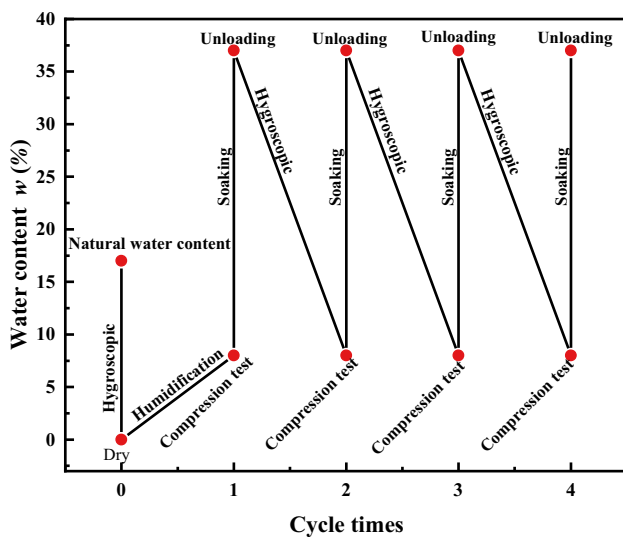


Fig. 3 Schematic diagram of the compression test process

were placed in a cool and dry place and were not exposed to the sun. When the water content in the sample reached the required value, the sample was placed in a sealed jar for at least 3 days. The test was performed in a timely manner after completing the sample preparation.

## Results and discussion

### Compression test results

It has been previously reported that compressive deformation and collapse deformation of loess can be transformed into each other under confined conditions. Therefore, the investigation of the compression deformation of loess with different water content is useful for further study of loess collapsibility. Therefore, the analysis first included a description of the stress–strain curves of loess with different water content, which were tested according to the schemes as shown in Fig. 3.

Figure 4 shows that the vertical strain ( $\epsilon$ ) of loess with different water content gradually increases with increasing vertical pressure ( $p$ ), while the final strain tended to stabilize. The strain value of the sample in the first compression was substantially higher than the value in the second compression, and with increasing compression time, the strain value of the sample with the same moisture content gradually decreased under the same pressure. After first collapse, the compression curves of the samples with different water content were distributed in a narrow range which indicates that the influence of the water content on the structure of samples decreased, i.e., the water sensitivity of the samples increased.

The slope of the  $e$ - $\lg p$  curve of loess increases gradually with increasing pressure (Fig. 5). The following formula is used to determine the void ratio for all samples:

$$e = e_0 - \epsilon(1 + e_0) \tag{1}$$

where  $\epsilon$  is the strain value of the sample, and  $e_0$  is the initial void ratio. Since this paper performed four compression tests,  $e_0$  is not a fixed value, but a void ratio at  $p = 0$  in each compression process.

When the load reaches a certain value, the compression curve will enter a straight-line stage, and its slope will remain unchanged. Before the  $e$ - $\lg p$  curve enters the straight-line stage, there will be a turning point in the curvature mutation. The load corresponding to the turning point is known as the compression yield strength, which is recorded as  $p_{sc}$  (Wang et al. 2019). Casagrande (1936) presented a method for determining the compressive yield strength. As can be noticed in Fig. 5, the straight part of the compression curve of some samples is not obvious. The  $p_{sc}$  of loess is

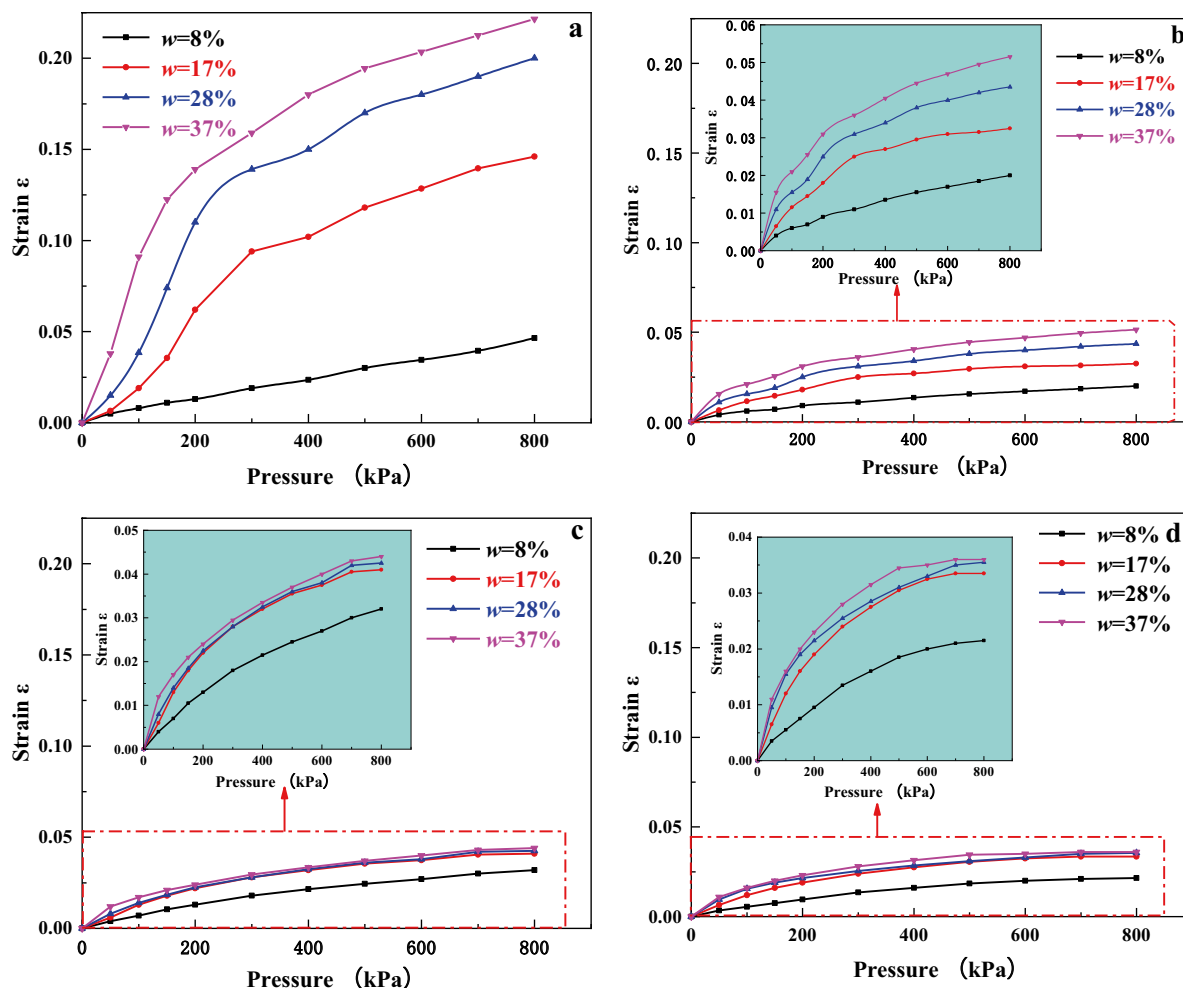


Fig. 4 Stress–strain curves: a first compression test, b second compression test, c third compression test, and d fourth compression test

obtained by the Casagrande method when the straight section of the curve is obvious; in case the straight section of the curve is not obvious,  $p_{sc}$  can be estimated according to the shape of the curve. However, this method is too complex to be applied for every compression curve. Therefore, in this study, an attempt was made to develop a simple method for obtaining the compressive yield strength. Structural strength is related to basic physical soil indices such as water content, void ratio, and particle size composition (Chen et al. 2011). Wang et al. (2019) proposed a comprehensive physical index, but neglected the influence of particle size composition on the structural strength of loess. Therefore, the present study defined a comprehensive physical index  $Z$  to represent the comprehensive physical properties of soil;  $Z$  is defined in Eq. (2):

$$Z = \frac{(w - w_p)\rho_d^2}{(w_l - w_p)\rho_{sat}\rho_w} \tag{2}$$

where  $w$ ,  $w_p$ ,  $w_l$ ,  $\rho_d$ ,  $\rho_{sat}$ , and  $\rho_w$  are water content, plastic limit, liquid limit, dry density, saturated density of loess, and water density, respectively.

The relationship curve between the compression yield strength and the comprehensive physical index  $Z$  is shown in Fig. 6.

Figure 6 shows that the initial compression yield strength and the recompression yield strength decrease exponentially with increasing the comprehensive physical index  $Z$ . The structural yield strength of the sample decreases with increasing water content (Yates et al. 2017). In addition, the slope of the curve decreases with increasing the comprehensive physical index  $Z$ , indicating that the water sensitivity of the sample decreases with increasing water content. Therefore, a simple method for calculating  $p_{sc}$  can be obtained, as shown in Eq. (3):

$$\begin{cases} p_{sc} = 141.85 \times \exp(-2.25 \cdot Z) + 46.71, \text{ for initial compression} \\ p_{sc} = 283.79 \times \exp(-0.98 \cdot Z) + 141.85, \text{ for recompression} \end{cases} \tag{3}$$

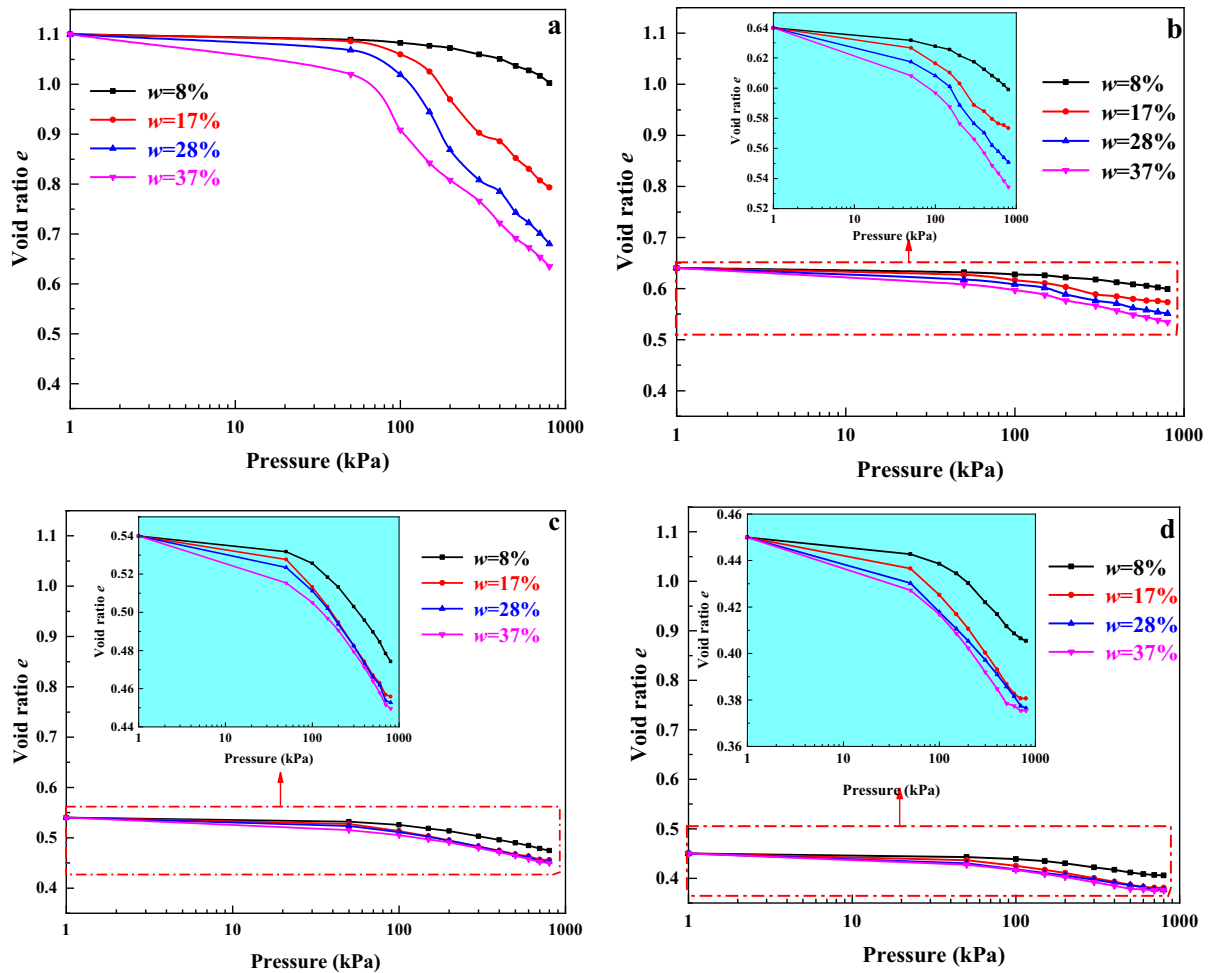


Fig. 5  $e - \lg p$  curves: **a** first compression test, **b** second compression test, **c** third compression test, and **d** fourth compression test

The Lanzhou  $Q_2$  loess data studied by Wang et al. (2019) are also shown in Fig. 6 for easier comparison. Equation (3) is still applicable to Lanzhou  $Q_2$  loess, but the  $P_{SC} - Z$  curve

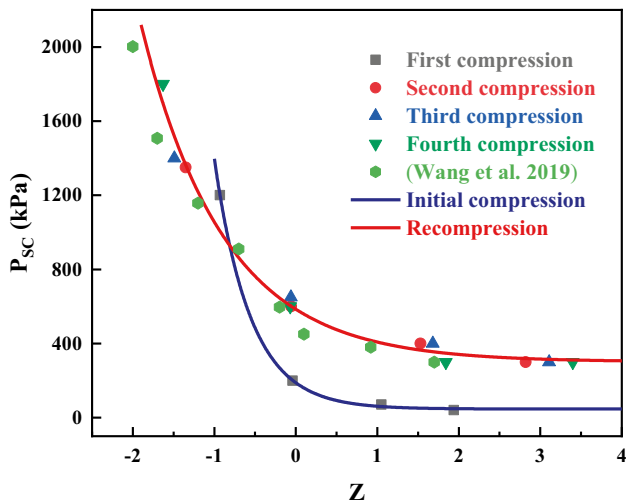


Fig. 6 Relationship curve between compression yield strength and the comprehensive physical index  $Z$

of  $Q_2$  loess is not the same as the  $P_{SC} - Z$  curve of  $Q_3$  loess initial compression. Even so, the  $P_{SC} - Z$  curve of  $Q_2$  loess still conforms to the  $P_{SC} - Z$  curve of recompression.

Using  $p/p_{sc}$  as the abscissa and logarithmic coordinates, the  $e - \lg(p/p_{sc})$  curves of the samples with different water content can be basically the same (Fig. 7).

As shown in Fig. 7, the  $e - \lg(p/p_{sc})$  curves of soil samples with different water content are distributed in a very narrow band and are approaching the same curve with the evident normalization effect; this indicates that a normalization effect will be observed for compression curves of samples with different water content. The new abscissa value corresponding to the turning point is  $p/p_{sc} = 1.0$ . As shown in Fig. 7, the  $e - \lg(p/p_{sc})$  curve of each test is essentially parallel. If the vertical coordinate (void ratio  $e$ ) in Fig. 7 is divided by the void ratio at the beginning of this experiment, the ordinate ( $\frac{e}{e_0}$ ) of the starting point (when  $p = 0$ ) of the curve becomes 1.0. Here,  $e_0$  is not a fixed value, yet a porosity ratio at  $p = 0$  in each compression process. When the curves of each test are drawn in the same coordinate system,

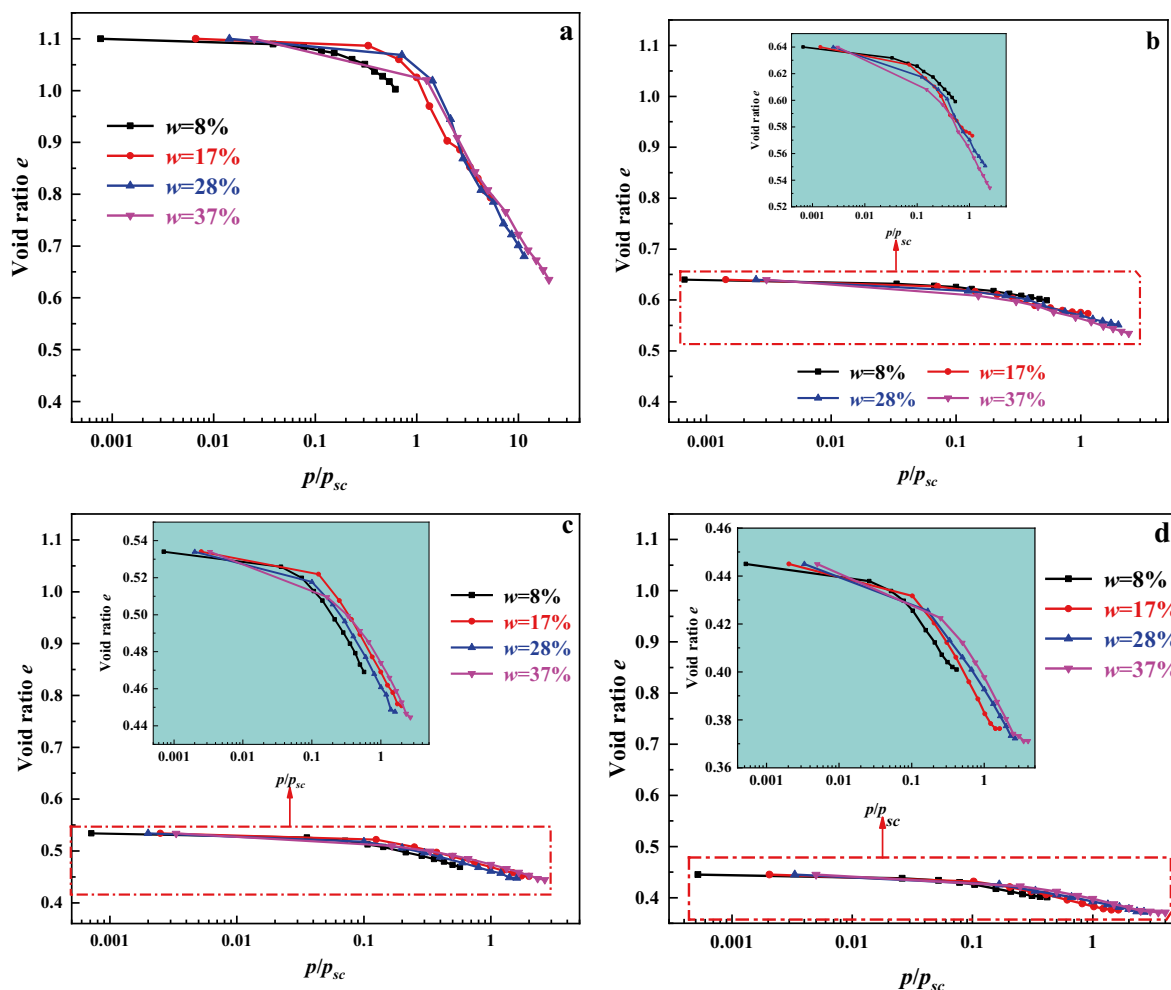


Fig. 7  $e-\lg(P/P_{sc})$  curves of undisturbed loess: **a** first compression test, **b** second compression test, **c** third compression test, and **d** fourth compression test

the  $(e/e_0) - \lg(p/p_{sc})$  curves of each test can be obtained (Fig. 8).

As seen in Fig. 8, the  $(e/e_0) - \lg(p/p_{sc})$  curves of loess with different test times almost coincide with one curve. This indicates that the normalization characteristics are shown not only on the compression curves of loess with different water content, but also on the compression curves of loess with different test times.

**Collapsibility evaluation based on the composite power exponential (CPE) nonlinear model**

The expression of the CPE nonlinear model can be used to describe all types of stress–strain curves. The stress–strain curves in the lateral compression test can be described as follows (Wang et al. 2017):

$$\varepsilon = n_0 \left\{ 1 - A \exp \left[ -\alpha \left( \frac{p}{p_a} \right)^\beta \right] \right\} \tag{4}$$

where  $p_a$  is the standard atmospheric pressure;  $n_0$  is the initial porosity;  $A$  is the coefficient related to the compression stage;  $\alpha$  and  $\beta$  are coefficients related to soil properties and water content, and their values are greater than 0.

Under the lateral limit condition, the compressive strain is  $\varepsilon = \frac{e_0 - e}{1 + e_0}$ , where  $e$  is the void ratio of the sample after the soil stabilizes under the vertical load  $p$  in the lateral limit condition. The compression strain  $\varepsilon = \frac{e_0 - e}{1 + e_0}$  and the void ratio formula  $n_0 = \frac{e_0}{1 + e_0}$  are introduced into Eq. (4), resulting in the following equation:

$$\frac{e}{e_0} = A \exp \left[ -\alpha \left( \frac{p}{p_a} \right)^\beta \right] \tag{5}$$

The abscissa of the curve in Fig. 7 is  $p/p_{sc}$ , and the ordinate is  $e/e_0$ ; therefore, it can be expressed by changing the form of Eq. (5), as follows:

$$\frac{e}{e_0} = A \exp\left[-\alpha \left(\frac{p}{p_{sc}}\right)^\beta\right] \tag{6}$$

Since both  $\alpha$  and  $\beta$  are greater than zero, Eq. (6) is a subtractive function. When  $p=0$ , then  $\frac{e}{e_0} = A$ , so the range of values of Eq. (6) is  $[A, 0)$ . With the increase in  $p$ , the void ratio begins to decrease from the initial void ratio; therefore, when  $p=0$ , then  $A = 1$ . Equation (6) can be used to fit the curve in Fig. 8, and the normalized curve expression shown in Fig. 8 is as follows:

$$\frac{e}{e_0} = \exp\left[-0.123 \left(\frac{p}{p_{sc}}\right)^{0.53}\right] \tag{7}$$

To verify the accuracy of the normalization method, the  $e$ - $\lg p$  compression curve was calculated according to the expression obtained from the normalization of the compression curve, and then compared with the  $e$ - $\lg p$  compression curve obtained from the experiment. The calculated  $e$ - $\lg p$  compression curve and the experimental  $e$ - $\lg p$  compression curve were plotted in the same coordinate system to verify the normalization characteristics of the compression curve. In this study, the compression curves of the four compression tests and the calculation for samples with a water content of 28% were compared (Fig. 9).

As shown in Fig. 9, except for the points under individual pressure, the calculated compression curve at different collapsing times was basically the same as the test compression curve, while the maximum deviation was not

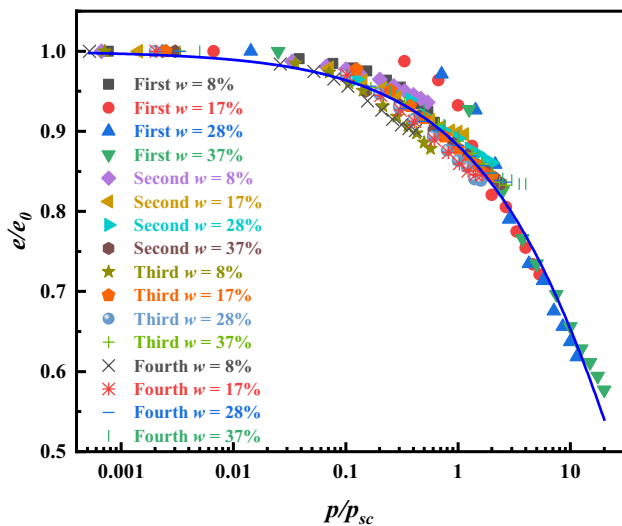


Fig. 8 ( $e/e_0$ )- $\lg(P/P_{sc})$  curves of undisturbed loess: first, second, third and fourth represent the first, second, third and fourth compression tests, respectively

more than 0.05, indicating that the normalization method was practical.

The collapsibility coefficient of loess can be expressed by  $\delta_s$ , and the calculation formula can refer to the specification (CNS, MOWR 2019) as follows:

$$\delta_s = \frac{h_p - h'_p}{h_0} \tag{8}$$

where  $h'_p$  is the height of the sample (in mm) at the appropriate stress level after inundation,  $h_p$  is the height of the sample (in mm) at the appropriate stress level before inundation, and  $h_0$  is the initial height of the sample (in mm).

The coefficient of collapsibility ( $\delta_s$ ) can be determined using Eq. (9):

$$\delta_s = \frac{e_p - e'_p}{1 + e_0} \tag{9}$$

where  $e_p$  and  $e'_p$  are the void ratios of the sample at the appropriate stress level before and after inundation, respectively; and  $e_0$  is the initial void ratio.

In order to calculate the collapsibility coefficient of loess with different water content and different collapsibility time, the physical parameters of soil samples are obtained by conventional geotechnical experiments. The comprehensive physical index  $Z$  of soil samples with different water content can be calculated according to the physical properties obtained experimentally, and  $p_{sc}$  can be calculated according to Eq. (3). Thereafter, the void ratio of soil samples with different water content under different pressures can be obtained according to Eq. (7) when the value of  $p_{sc}$  is known. Finally, the collapsibility coefficients of samples with different water content under different pressures can

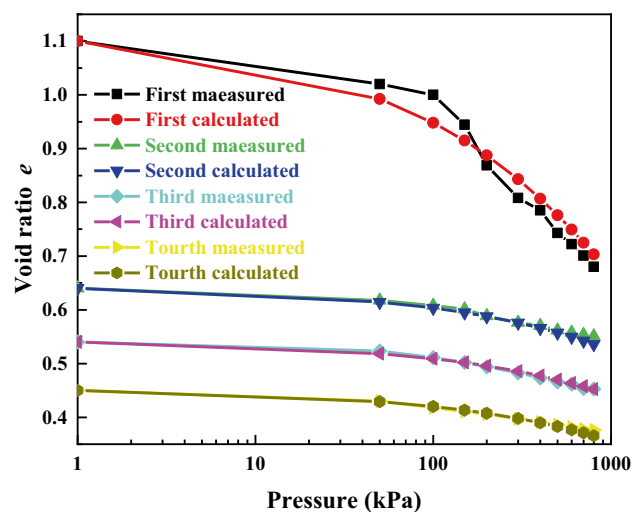


Fig. 9 Comparison between the calculated compression curve and the measured compression curve of loess

be calculated using Eq. (9) and the initial pore ratio. The method can be used to obtain the collapsibility coefficients of samples with different moisture content under different pressures based on the physical parameters of the samples, which substantially simplifies geotechnical experiments.

Figure 10 shows the collapsibility coefficients of samples with different water content obtained by the aforementioned method. As the pressure increases, the collapsibility coefficient firstly increases, then decreases, and finally stabilizes. The maximum collapsibility coefficient is observed under different pressures, and it can be called the peak collapsibility coefficient, while the corresponding pressure represents the peak collapsibility pressure. The peak collapsibility coefficient and the peak collapsibility pressure decrease with increasing water content. The reason for this phenomenon is that when the pressure is lower than the peak collapse pressure, the unsaturated sample cannot be completely compressed as the matrix suction and cementation material

strength can maintain the upper load stability. However, the salt in the saturated sample dissolves, resulting in an increase in the internal pore diameter and a decrease in the matrix suction; thus, the strength of the sample is reduced and leads to a greater collapse (Haeri et al. 2013; Mihalache and Buscarnera 2015). When the pressure exceeds the peak collapse pressure, the unsaturated sample cannot bear the load, resulting in damage to the soil sample structure. However, the structure of the saturated sample is destroyed under low pressure. Therefore, when the pressure exceeds the peak collapse pressure, the collapsibility coefficient decreases with increasing pressure. Similarly, as the water content increases, part of the cementation material in the sample dissolves and the matrix suction decreases. Under low pressure, the structure of the sample can be destroyed, and thus, the peak collapsibility pressure decreases with increasing water content.

The initial collapse pressure is the vertical pressure corresponding to a collapsibility coefficient of 0.015, which

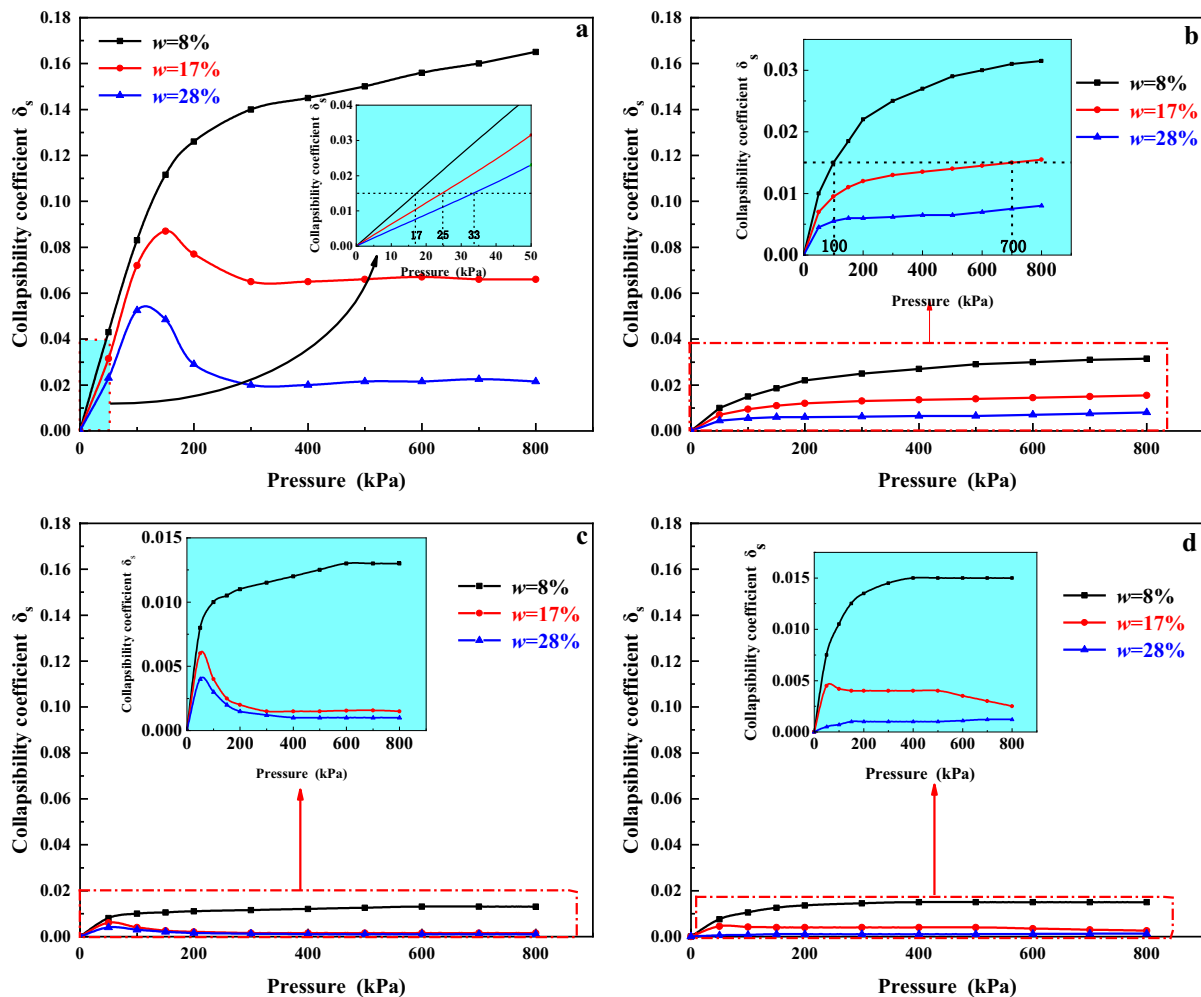


**Fig. 10** Collapsibility coefficient of loess samples with different water content: **a** first compression test, **b** second compression test, **c** third compression test, and **d** fourth compression test



reflects the ability of the loess to resist collapse. The initial collapsibility pressures of the three samples with different water content during the first collapse were 17 kPa, 25 kPa, and 33 kPa, respectively. The initial collapsibility pressure increases with increasing moisture content in the sample, indicating that samples with lower moisture content are more prone to collapse. As the collapse time increases, the initial collapsibility pressure gradually increases, while the peak collapsibility coefficient greatly decreases. After collapsing two times, the sample has no collapsibility. This indicates that the collapsibility of the loess foundation cannot be completely eliminated after one collapse, but collapsibility gradually reduces with repeated collapses.

### Description of the evaluation method

The demolition and reconstruction of old buildings caused by the construction of the sponge city will cause the repeated collapse of the loess foundation. At present, studies on the repeated collapsibility of loess are rare, and there is no recognized method for evaluating the repeated collapsibility of loess. In this paper, a method for evaluating the repeated collapsibility of loess is proposed based on the test data. This method links the structural yield strength of loess with the basic physical index of loess and proposes an empirical formula for calculating the structural yield strength. Therefore, this method can complete the repeated collapsibility evaluation of loess through basic physical indicators and simple testing instruments. Since the basic physical index of loess is affected by its stress history, the compression curve of loess samples that have experienced collapse is affected by the previous collapse pressure. To investigate the law of repeated collapse, the collapse pressure used is 800 kPa, but in reality, the building load varies greatly. The applicability of Eq. (7) under any pressure has yet not been evaluated, but the method of the evaluation of repeated collapsibility proposed in this paper is still applicable for the evaluation of repeated collapsibility under other pressures, thereby representing a reference method for the study of repeated collapsibility of loess.

### Conclusions

In this study, repeated compression tests on soil samples with different water content yielded a compression curve of loess in Guyuan. First, a comprehensive physical index is defined based on the three main parameters (moisture content, void ratio, and particle size composition) that affect the loess structure. The relationship between the comprehensive physical index and the structural yield strength of loess for the repeated collapsibility was then explored. Finally, based on the analysis of the characteristics of repeated collapsibility of loess, this paper proposes a simple and easy method

for evaluating the repeated collapsibility of loess. The specific conclusions of this study are as follows:

1. The yield strength of structure decreases rapidly with increasing the comprehensive physical index  $Z$  and decreases along the same path with increasing the comprehensive physical index in the second, third, and fourth collapse. For collapse times, the yield strength of the structure decreases with increasing water content. The slope of the curve between the structural yield strength and the comprehensive physical index  $Z$  decreases with increasing the comprehensive physical index  $Z$ , indicating that the water sensitivity of the sample decreases with increasing water content;
2. Not only do the compression curves of loess with different water content have normalization characteristics, but also the compression curves of loess with different test times have normalization characteristics;
3. The new evaluation method of repeated collapsibility of loess only needs the basic physical index of loess; a simple compression test can be performed quickly to obtain the collapsibility coefficient of loess with different water content and collapsible times
4. Comparing the calculated compression curve and the measured compression curve of the sample with a water content of 28%, the maximum error of the void ratio was less than 0.05, indicating a good accuracy of this method;
5. The collapse is not completed in one step. Actually, the loess with a moisture content of  $< 17\%$  collapses do exist repeated collapse, and for twice. The coefficient of collapsibility decreases rapidly with increasing collapse time, while the ability of loess to resist collapse increases.

**Funding** The research work of this paper is supported by the fund “Research on key technologies for construction and operation of Guyuan sponge city” (No. schm-2018–0302).

### References

- ASTM International (2003) ASTM D5333–03. Standard test method for measurement of collapse potential of soils. ASTM International, West Conshohocken, PA
- Casagrande A (1936) The determination of pre-consolidation load and its practical significance. Proceedings of the 1st International Conference on Soil Mechanics and Foundation Engineering 3:93–108
- Chen X, Luo YS, Cheng DW, Guo H (2011) Experimental study of loess structural strength and resistance coefficient. *Appl Mech Mater* 90:98–107. <https://doi.org/10.4028/www.scientific.net/AMM.90-93.98>
- CNS, Mowr (2019) GB/T50123-2019. Standard for geotechnical testing method. China Planning Press, Beijing in Chinese
- Delage P, Audiguier M, Cui Y, Howat MD (1996) Microstructure of a compacted silt. *Can Geotech J* 33(1):150–158. <https://doi.org/10.1139/t96-030>

- Dijkstra TA (2001) Geotechnical thresholds in the Lanzhou loess of China. *Quatern Int* 76–77(1):21–28. [https://doi.org/10.1016/S1040-6182\(00\)00086-0](https://doi.org/10.1016/S1040-6182(00)00086-0)
- Gao G (1988) Formation and development of the structure of collapsing loess in China. *Eng Geol* 25(2–4):235–245. [https://doi.org/10.1016/0013-7952\(88\)90029-4](https://doi.org/10.1016/0013-7952(88)90029-4)
- Haeri SM, Garakani AA, Khosravi A, Meehan CL (2013) Assessing the hydro-mechanical behavior of collapsible soils using a modified triaxial test device. *Geotech Test J* 37. <https://doi.org/10.13140/2.1.4288.1608>
- Hao Q, Guo Z, Qiao Y, Xu B, Oldfield F (2010) Geochemical evidence for the provenance of middle Pleistocene loess deposits in southern China. *Quat Sci Rev* 29:3317–3326. <https://doi.org/10.1016/j.quascirev.2010.08.004>
- Jiang M, Zhang F, Hu H, Cui Y, Peng J (2014) Structural characterization of natural loess and remolded loess under triaxial tests. *Eng Geol* 181:249–260. <https://doi.org/10.1016/j.enggeo.2014.07.021>
- Kim D, Kang S (2013) Engineering properties of compacted loesses as construction materials. *KSCE J Civ Eng* 17(2):335–341. <https://doi.org/10.1007/s12205-013-0872-1>
- Li Y (2018) A review of shear and tensile strengths of the Malan Loess in China. *Eng Geol* 236:4–10. <https://doi.org/10.1016/j.enggeo.2017.02.023>
- Liang C, Cao C, Wu S (2018) Hydraulic-mechanical properties of loess and its behavior when subjected to infiltration-induced wetting. *Bull Eng Geol Environ* 77:385–397. <https://doi.org/10.1007/s10064-016-0943-x>
- Liu Y, Cao GZ, Meng YG, Liu MX (2013) Study on the microstructure feature and strength mechanism of the Tien Lake Peat Soil. *Adv Mater Res* 864:2695–2702. <https://doi.org/10.4028/www.scientific.net/AMR.864-867.2695>
- Lutenegger AJ (1981) Stability of loess in light of the inactive particle theory. *Nature* 291:360. <https://doi.org/10.1038/291360a0>
- Lv Q, Wang S, Wang D, Wu Z (2014) Water stability mechanism of silicification grouted loess. *Bull Eng Geol Environ* 73(4):1025–1035. <https://doi.org/10.1007/s10064-014-0646-0>
- Mei Y, Li Y, Wang X, Wang J, Hu C (2019) Statistical analysis of deformation laws of deep foundation pits in collapsible loess. *Arab J Sci Eng* 44(10):8347–8360. <https://doi.org/10.1007/s13369-019-03931-6>
- Mihalache C, Buscarnera G (2015) Is wetting collapse an unstable compaction process? *J Geotech Geoenviron Eng* 141(2):420–432. [https://doi.org/10.1061/\(ASCE\)GT.1943-5606.0001226](https://doi.org/10.1061/(ASCE)GT.1943-5606.0001226)
- Rogers CDF, Dijkstra TA, Smalley IJ (1994) Hydroconsolidation and subsidence of loess: studies from China, Russia, North America and Europe: In memory of Jan Sajgalik. *Eng Geol* 37(2):83–113. [https://doi.org/10.1016/0013-7952\(94\)90045-0](https://doi.org/10.1016/0013-7952(94)90045-0)
- Romero E, Simms PH (2008) Microstructure investigation in unsaturated soils: a review with special attention to contribution of mercury intrusion porosimetry and environmental scanning electron microscopy. *Geotech Geol Eng* 26(6):705–727. <https://doi.org/10.1007/s10706-008-9204-5>
- Shao X, Zhang H, Tan Y (2018) Collapse behavior and microstructural alteration of remolded loess under graded wetting tests. *Eng Geol* 233:11–22. <https://doi.org/10.1016/j.enggeo.2017.11.025>
- Sun JZ, Liu JM (2000) On unsaturated collapse, remnant collapse and multiple collapse of the loess. *Chin J Geotech Eng* 22(03):365–367 (In Chinese)
- Wang L, Lu ZG, Shao S (2017) A composite power exponential nonlinear model of rock and soil. *Chin J Rock Mechan Eng* 36(05):1269–1278
- Wang L, Shao S, She F (2019) A new method for evaluating loess collapsibility and its application. *Eng Geol* 264:105376. <https://doi.org/10.1016/j.enggeo.2019.105376>
- Xie WL, Li P, Zhang MS, Cheng TE, Wang Y (2018) Collapse behavior and microstructural evolution of loess soils from the Loess Plateau of China. *J Mt Sci-Engl* 15(8):1642–1657. <https://doi.org/10.1007/s11629-018-5006-2>
- Xie X, Qi S, Zhao F, Wang D (2017) Creep behavior and the microstructural evolution of loess-like soil from Xi'an area, China. *Eng Geol* 236:43–59. <https://doi.org/10.1016/j.enggeo.2017.11.003>
- Yates K, Fenton CH, Bell DH (2017) A review of the geotechnical characteristics of loess and loess-derived soils from Canterbury, South Island, New Zealand. *Eng Geol* 236:11–22. <https://doi.org/10.1016/j.enggeo.2017.08.001>
- Yuan ZX, Wang LM (2009) Collapsibility and seismic settlement of loess. *Eng Geol* 105:119–123. <https://doi.org/10.1016/j.enggeo.2008.12.002>